https://doi.org/10.5194/egusphere-2024-1325
Preprint. Discussion started: 22 May 2024

Molecular and seasonal characteristics of organic vapors in urban Beijing: insights from Vocus-PTR measurements

Zhaojin An[1,2], Rujing Yin[3], Xinyan Zhao[1], Xiaoxiao Li[4], Yi Yuan[1], Junchen Guo[1], Yuyang Li[1], Xue Li[5], Dandan Li[1], Yaowei Li[2], Dongbin Wang[1], Chao Yan[6], Kebin He[1], Douglas R. Worsnop[7,8], Frank N. Keutsch[2], Jingkun Jiang[1,*]

[1]State Key Joint Laboratory of Environment Simulation and Pollution Control, School of Environment, Tsinghua University, 100084, Beijing, China

[2]School of Engineering and Applied Sciences, Harvard University, Cambridge, Massachusetts 02138, USA

[3]Key Laboratory of Industrial Ecology and Environmental Engineering (Ministry of Education), School of Environmental Science and Technology, Dalian University of Technology, 116024, Dalian, China

[4]School of Resource and Environmental Sciences, Wuhan University, 430072, Wuhan, China

[5]School of Environment, Henan Normal University, 453007, Xinxiang, China

[6]Joint International Research Laboratory of Atmospheric and Earth System Research, School of Atmospheric Sciences, Nanjing University, 210023, Nanjing, China

[7]Institute for Atmospheric and earth System Research / Physics, Faculty of Science, University of Helsinki, Helsinki 00014, Finland

[8]Aerodyne Research, Inc., Billerica, Massachusetts 01821, USA

*Corresponding author: Jingkun Jiang (email: jiangjk@tsinghua.edu.cn)

https://doi.org/10.5194/egusphere-2024-1325
Preprint. Discussion started: 22 May 2024

Abstract

Understanding the compositions and evolution of atmospheric organic vapors is crucial for exploring their impact on air quality. However, the molecular and seasonal characteristics of organic vapors in urban areas, with complex anthropogenic emissions and high variability, remain inadequately understood. In this study, we conducted measurements in urban Beijing during 2021-2022 covering four seasons using a Vocus-PTR, an improved Proton Transfer Reaction-Mass Spectrometry (PTR-MS). During the measurement period, a total of 895 peaks are observed, and 543 of them can be assigned to formulas. The contribution of $C_xH_yO_z$ species is most significant, which compose up to 53.7% of the number and 76.0% of the mass of total organics. With enhanced sensitivity and mass resolution, various sub-ppt level species and organics with multiple oxygens (≥3) were discovered. When counting the species number, 42.2% of the organics measured are at sub-ppt level and 37.8% of the species contain 3-8 oxygens. Organic vapors with multiple oxygens mainly consist of intermediate volatility and semi-volatile compounds, and many of them are found to be the multi-generational oxidation products of various volatile organic precursors. In summer, the fast photooxidation process generates organic vapors with multiple oxygens, and leads to an increase in both their concentration and proportion. While in other seasons, the variations of organic vapors with multiple oxygens are closely correlated with those of organic vapors with 1-2 oxygens, which could be heavily influenced by primary emissions. Organic vapors with low oxygen content (≤ 2 oxygens) are comparable to the results obtained by traditional PTR-MS measurements in both urban Beijing and neighboring regions.

https://doi.org/10.5194/egusphere-2024-1325
Preprint. Discussion started: 22 May 2024

1 Introduction

Volatile organic compounds (VOCs) play a crucial role in the formation of ozone and $PM_{2.5}$ (particulate matter with an aerodynamic diameter equal to or less than 2.5 μm) in the atmosphere, subsequently affecting air quality, climate, and human health (Carter, 1994; Williams and Koppmann, 2007; Jimenez et al., 2009; Hallquist et al., 2009). The sources and atmospheric evolution of VOCs in the atmosphere are complex due to the coexistence of compounds from primary emissions as well as secondary formation (Gentner et al., 2013; Gilman et al., 2015; Millet et al., 2015). Understanding their molecular characteristics is essential for studying their hydroxyl radial (OH) reactivities, ozone and secondary organic aerosol (SOA) formation potentials, especially for oxygenated VOCs (OVOCs) with low volatility that may directly partition to aerosols. However, the diverse range of species and wide distribution of oxidation products of atmospheric VOCs make it challenging to unravel their molecular properties (Goldstein and Galbally, 2007).

Instrumental advances have allowed for improving the understanding of the compositions and variations of VOCs at the molecular level, especially for OVOCs. Gas chromatography or multidimensional gas chromatography coupled with mass spectrometry is the most commonly used technology for VOC measurement, capable of detecting major non-methane hydrocarbons and select OVOCs (Lewis et al., 2000; Xu et al., 2003; Noziere et al., 2015). Proton Transfer Reaction-Mass Spectrometry (PTR-MS) enables real-time detection of VOCs without pre-concentration and separation. In PTR-MS, VOCs are ionized via proton transfer by hydronium ions (H_3O^+) in the ion-molecule reactor (IMR) (Hansel et al., 1995; Yuan et al., 2016). The sensitivity can be quantified based on the proton transfer reaction rate while simultaneously considering ion transmission, detector efficiency, etc. (Cappellin et al., 2012; Jensen et al., 2023). PTR-MS has greatly enriched the molecular understanding of OVOCs due to its high sensitivity to oxygen-containing compounds (Hansel et al., 1995; De Gouw and Warneke, 2007; Yuan et al., 2017). The use of time-of-flight (TOF) mass analyzers has greatly improved the isobaric mass resolving power of PTR-MS, compared to the traditionally used quadruple analyzers (Jordan et al., 2009; Graus et al., 2010). Hundreds of OVOCs are detected and characterized in different areas using PTR-MS, e.g. urban (Wu et al., 2020), suburban (He et al., 2022), and forest areas (Pugliese et al., 2023).

Recent developments in the IMR configuration have greatly increased sensitivities and concurrently lowered the limits of detection of PTR-MS by several orders of magnitude. PTR3 promotes the product ion formation by increasing the reaction time and pressure in the IMR (Breitenlechner et al., 2017). Vocus-PTR improves the transmission in the IMR by incorporating radio

https://doi.org/10.5194/egusphere-2024-1325
Preprint. Discussion started: 22 May 2024

frequency electric fields to focus ions (Krechmer et al., 2018). FUSION PTR-TOF enhances the IMR with a static longitudinal electric field stacked by a focusing transversal radiofrequency field to achieve ultrasensitive detection (Reinecke et al., 2023). These improvements have expanded the detection capabilities of PTR-MS, particularly for organic vapors with low concentrations, lower volatility, and multiple oxygens (≥3) (Riva et al., 2019). This enables the simultaneous measurement of VOC precursors and their primary, secondary, and higher-level oxidation products using a single instrument (Li et al., 2020), facilitating the study of atmospheric chemical evolution of organics (Wang et al., 2020a).

These improved PTR-MS systems have gradually gained traction in research applications over the past few years, including measuring organics in controlled lab studies (Zaytsev et al., 2019a; Zaytsev et al., 2019b; Riva et al., 2019; Li et al., 2022a; Li et al., 2024), emission sources (Sreeram et al., 2022; Yu et al., 2022; Yacovitch et al., 2023; Wohl et al., 2023; Jahn et al., 2023), and ambient air. For ambient measurements, observations in forested regions have been extensively conducted to study the compositions, variations, fluxes, and emissions of organics from different plants (Li et al., 2020; Li et al., 2021; Huang et al., 2021; Fischer et al., 2021; Thomas et al., 2022; Vettikkat et al., 2023; Vermeuel et al., 2023). Terpenes and their oxidation products with oxygen number up to 6 have been detected. Diterpenes have been directly observed in the ambient air for the first time owing to the substantial improvement in sensitivity of Vocus-PTR. Ambient measurement has been also conducted on a mountain in China, which found that terpenes and their oxidation products dominate the detected organic compounds, while the influence of industrial emissions can also be observed (Zhang et al., 2024).

In urban atmospheres, the sources and evolution of VOCs are considerably complex, potentially exhibiting distinct characteristics compared to forested areas. The current applications of these improved PTR-MS in urban air are limited. Jensen et al. (2023) conducted a one-month observation to address the production of reliable measurements. A few low-signal species including dimethylamine, icosanal, dimethyl disulfide, and siloxanes emitted from diverse emission sources have been detected as a result of the enhanced sensitivity (Wang et al., 2020b; Chang et al., 2022; Jensen et al., 2023). Due to the relatively sparse deployment of these improved PTR-MS systems in urban environments, the understanding of organic vapors with low mixing ratios in urban air, including their species, concentrations, diurnal profiles, and seasonal variations, remains inadequate.

In this study, we conducted measurements of organic vapors using a Vocus-PTR in urban Beijing during 2021-2022, covering four seasons. We present general characteristics of measured organic vapors and compare them with traditional PTR-MS and previous Vocus-PTR measurements. We focus on

https://doi.org/10.5194/egusphere-2024-1325
Preprint. Discussion started: 22 May 2024

organic vapors with multiple oxygens (three or more), which have rarely been individually analyzed at molecular level in previous studies due to their low mixing ratios. Their chemical compositions, atmospheric concentrations, diurnal and seasonal variations are reported. Cluster analysis is further conducted to resolve the main driving factors of their variations.

2 Methods

2.1 Measurements

The observation site is located in the central area of Tsinghua University, Beijing (40°0'N, 116°20'E), approximately 1 kilometer from nearby traffic roads (Fig. S1 in the supporting information, SI). It is an urban site with no significant direct influence from industrial activities or heavy-traffic arteries. Details of this site can be found in the previous study (Cai and Jiang, 2017). Organic vapors were measured by a Vocus-2R PTR-TOF-MS (Tofwerk AG and Aerodyne Research Inc., referred to as Vocus-PTR hereinafter), which was situated on top of a fourth-floor tower building, with its sampling inlet positioned approximately 20 meters above the ground. The observation period was from May 1st, 2021 to March 10th, 2022, covering four seasons. Detailed information about observation periods and their corresponding seasons is shown in Table S1.

The operating parameters of the Vocus-PTR used in this study are briefly described here (Krechmer et al., 2018). The ion source was supplied with a water vapor flow of 20 sccm. The IMR was operated at 100°C and 2 mbar with axial voltage of 600 V and quadrupole amplitude voltage of 450 V. The IMR operating parameters were optimized to minimize the formation of water clusters. Mass spectra were collected from m/z 11 to m/z 398 with a time resolution of 5 s, achieving a mass resolution ~10,000 for $C_7H_9^+$ throughout the measurement period. Ambient air was sampled via a tetrafluoroethylene (PTFE) tube (1.35 m long, 1/4-inch OD) at a flow rate of 3 LPM to reduce wall losses, with only 150 sccm flow entering the Vocus-PTR. A regularly replaced Teflon filter was used in front of the sampling line to remove particles. Measurements were made on a 2-hour cycle with 110 min for ambient air, 5 min for zero gas, and 5 min for fast calibration. The fast calibrations involved the use of mixed calibration gases containing 13 VOCs. Detailed information about these calibration gases can be found in Table S2.

The $PM_{2.5}$, NO_2, and O_3 data are obtained from a state-operated air quality station (Wanliu station), located approximately 5.6 km away from our observation site. The meteorological parameters, including temperature (T), relative humidity (RH), wind speed, and wind direction are also obtained from Wanliu station. The diurnal variations of $PM_{2.5}$, O_3, NO_x, RH, and T in four seasons are shown in Figure S2.

https://doi.org/10.5194/egusphere-2024-1325
Preprint. Discussion started: 22 May 2024

2.2 Data processing

Data analysis of Vocus-PTR mass spectra, including mass calibration, baseline subtraction, and high-resolution peak fitting was conducted using Tofware (v3.2.3, Tofwerk AG and Aerodyne Research Inc.) within the Igor Pro 8 platform (WaveMetrics, OR, USA). Determination of sensitivities and cluster analysis were performed in MATLAB R2022a (The MathWorks Inc., USA).

In PTR-MS, the sensitivities of organic vapors are typically determined through their direct linear correlation with their PTR rate constant (k_{PTR}). Vocus-PTR utilizes a big segmented quadrupole with a high-pass band filter, which detects ions <35 m/z with reduced transmission efficiency (Krechmer et al., 2018). Consequently, determining sensitivities in Vocus-PTR involves consideration of both reaction efficiency and transmission efficiency. The average sensitivities of mixed calibration gases were used to set up a linear relationship between k_{PTR} and sensitivities, taking into account the transmission efficiency curve during each observation period. Figure S3a shows the measured sensitivities of mixed calibration gases and their corresponding k_{PTR} values. Ions $C_7H_9^+$, $C_8H_{11}^+$, and $C_9H_{13}^+$ have the steepest slopes and are minimally affected by reduced transmission efficiency. Thus, the average slope of these ions was used to determine the linear correlation between sensitivity and k_{PTR}. Sensitivities of other ions in mixed calibration gases may be influenced by transmission and fragmentation. The transmission efficiency of mixed calibration gases was calculated using sensitivities of mixed calibration gases and average slope of $C_7H_9^+$, $C_8H_{11}^+$, and $C_9H_{13}^+$, as shown in Figure S3b. The transmission efficiency of mixed calibration gases closely aligns with the fitted transmission efficiency curve, except for $C_{10}H_{17}^+$ which potentially experiences fragmentation. For organic vapors without standards, their theoretical k_{PTR} were used to calculate sensitivities, while for organic vapors with no theoretical k_{PTR}, an average k_{PTR} of known species, 2.5×10^{-9} cm^3/s was used to determine their sensitivities. The theoretical k_{PTR} of organic vapors are obtained from previous studies (Zhao and Zhang, 2004; Cappellin et al., 2012; Sekimoto et al., 2017).

Double bond equivalent (DBE), carbon oxidation state ($\overline{OS}_C$), and volatility of organic vapors are calculated to address their chemical and physical properties. DBE is calculated as follows:

$$DBE = n_C + 1 - 0.5 \times n_H + 0.5 \times n_N \quad (1)$$

Where n_C, n_H, and n_N are the number of carbon, hydrogen, and nitrogen atoms of organic vapors, respectively. $\overline{OS}_C$ is calculated as follows (Kroll et al., 2011):

$$\overline{OS}_C = 2 \times n_O/n_C - n_H/n_C \quad (2)$$

Where n_C, n_O, and n_H are the number of carbon, oxygens, and hydrogen atoms of organic vapors, respectively. The saturation mass concentration C_0, calculated using parameterization method by Li et al. (Li et al., 2016), are used

https://doi.org/10.5194/egusphere-2024-1325
Preprint. Discussion started: 22 May 2024

to describe the volatility of organic vapors, as given below:

$$log_{10}C_0 = (n_C^0 - n_C)b_c - n_O b_O - 2\frac{n_C n_O}{n_C + n_O} b_{CO} - n_N b_N \quad (3)$$

Where n_C^0 is the reference carbon number; n_C, n_O, and n_N are the number of carbon, oxygen, and nitrogen atoms of organic vapors, respectively; b_c, b_O, and b_N are the contribution of carbon, oxygen, and nitrogen atom to $log_{10}C_0$, respectively; b_{CO} is the carbon-oxygen nonideality.

Quantified concentrations are further processed by cluster analysis to investigate their characteristics. Intraclass correlation coefficient (ICC) combined with k-means cluster analysis are used. ICC is a suitable method for assessing the consistency of trends in unbalanced data. It quantifies the stability of differences between two sets of measurement results, enabling evaluation of their consistency. ICC(C, 1) is selected among several typical consistency evaluation parameters for its evaluation results exhibit the highest level of differentiation based on factual evidence (Qiao et al., 2021). ICC(C, 1) is calculated as follows:

$$ICC(C,1) = (D(X+Y) - D(X-Y))/(D(X+Y) + D(X-Y)) \quad (3)$$

where $D(\cdot)$ is the arithmetic operators of variance. X and Y are two sets of measurement data, in this case referring to the concentrations of any organic vapors we are concerned about. The ICC matrices of various organic vapors are subsequently utilized as input for k-means analysis. Sqeuclidean distance is selected to calculate the distances between different organic vapors.

3 Results and discussion

3.1 General characteristics of organic vapors

During the measurement period, a total of 895 peaks are observed, and 543 of them can be assigned to formulas, divided into C_xH_y, $C_xH_yO_z$, $C_xH_yN_i$, and $C_xH_yO_zN_i$ categories based on their elemental compositions (Fig. 1a). $C_xH_yO_z$ species compose up to 53.7% of the total number of organics followed by $C_xH_yO_zN_i$, C_xH_y, and $C_xH_yN_i$, with proportions of 26.3%, 14.4%, and 5.6%, respectively (Fig. 1b). $C_xH_yO_z$ species dominate contributing 76.0% of the annual median concentrations of total organics, followed by $C_xH_yO_zN_i$, C_xH_y, and $C_xH_yN_i$, with proportions of 18.7%, 3.4%, and 1.9%, respectively (Fig. 1c). In addition to these resolved formulas, we also detect 18 peaks containing other elements such as S, Cl, Si, etc., and 79 CH(O)(N) peaks that do not comply with nitrogen rules, which we consider as fragments or free radicals. There are 228 unknown peaks for which formulas cannot be assigned. The concentrations of organic vapors vary significantly in urban Beijing, ranging from 0.01 parts per trillion (ppt) to 10 parts per billion (ppb), with many species detected at sub-ppt levels notably (Fig. 1d). As the molecular masses of organics increase, their

https://doi.org/10.5194/egusphere-2024-1325
Preprint. Discussion started: 22 May 2024

annual median concentrations decrease. The concentrations of $C_xH_yO_z$ and $C_xH_yO_zN_i$ categories start to decrease below the ppt level above molecular weights of 160 and 125, respectively.

With enhanced sensitivity and mass resolution, an increased number of species have been discovered compared to traditional PTR-MS measurements in urban Beijing, especially compounds with lower concentrations and higher oxygen contents. Note that most organics with low concentrations have high oxygen content. 42.2% organics in number measured in this study are at sub-ppt level while 30.7% in number are between 1 and 10 ppt (Fig. 1e). Only compounds detected above ppt levels were previously reported in urban sites within Beijing (Sheng et al., 2018; Li et al., 2019), as well as at a suburban site located 100 km southwest of Beijing (He et al., 2022). Simultaneously, organic vapors with multiple oxygens ($C_xH_yO_{\geq 3}$ and $C_xH_yO_{\geq 3}N_i$ species) have been successfully detected in this study in the urban atmosphere. Traditionally, they have been often recognized as total $C_xH_yO_{\geq 3}$ species, with no individually analysis in traditional PTR-MS (Yuan et al., 2023; Li et al., 2022b; He et al., 2022). Many other studies only focus on reporting OVOCs containing up to 2-3 oxygens or omit to address the presence of nitrogen containing OVOCs (Wang et al., 2021; Liu et al., 2022). The low mixing ratios and high wall losses of organic vapors with multiple oxygens impact the detection in traditional PTR-MS (Breitenlechner et al., 2017). Figure 2a reinterprets the mass defect plot of measured organics with a focus on oxygen numbers, ranging from 0 to 8. The analysis of concentration levels and variations of organic vapors with multiple oxygens (≥3) are shown in Section 3.2. Organic vapors with low oxygen content (≤2) are reported in Section 3.3. Subsequent comparison of Vocus-PTR and traditional PTR in urban Beijing and both Vocus-PTR measurements in urban Beijing and European forests are also shown in Section 3.3.

3.2 Organic vapors with high oxygen content

197 observed organics with multiple oxygen atoms account for 37.8% in number of the total organic compounds, including 137 species of $C_xH_yO_{\geq 3}$ and 60 species of $C_xH_yO_{\geq 3}N_i$. Organics with oxygen numbers 3 and 4 dominates within the $C_xH_yO_{\geq 3}$ and $C_xH_yO_{\geq 3}N_i$ species (Fig. 2b and Fig. 2c). Compounds with oxygen number of 3, 4, 5, and ≥6 comprise 15.5%, 11.0%, 6.8%, and 5.4% of the total species number of $C_xH_yO_z$ compounds, respectively. While compounds with oxygen number of 3, 4, 5, and ≥ 6 comprise 15.7%, 11.4%, 7.2%, and 1.8% of the total species number of $C_xH_yO_zN_i$ compounds, respectively.

The measured organic vapors with multiple oxygens are mainly intermediate volatile organic compounds (IVOCs) and semi-volatile organic compounds (SVOCs). The dominant carbon numbers range from 5 to 9 and DBE between 1-5, accounting for over three-quarters of the total species number of organic

https://doi.org/10.5194/egusphere-2024-1325
Preprint. Discussion started: 22 May 2024

vapors with multiple oxygens (Fig. 3a and Fig. 3b). The maximum occurrence of organic vapors with 3 or 4 oxygen atoms is observed within the carbon range of 7-8 and a DBE value of 2. For organic vapors species with 5 or more oxygens, they reach their peak at a smaller carbon number of 4-5 and a higher DBE value of 3. This indicates that the main chemical transformation of organic vapors with multiple oxygens are functionalization and fragmentation reactions (Kroll et al., 2011; Isaacman-Vanwertz et al., 2018), also shown in Figure S4. Based on calculated volatility, 80% of the species are IVOCs, and the remaining 20% are SVOCs (Fig. 3c). With the increase in oxygen number, the volatility of the compounds gradually decreases, while the potential partitioning to aerosols increases, manifested by a gradual reduction in the peak values of the $log_{10}C_0$. Compounds containing nitrogen, referred to shaded bars with white stripes in Figure 3c, have a lower volatility compared to non-nitrogen species.

The annual concentration of measured organic vapors with multiple oxygens in mean ± standard deviation is 2754 ppt ± 1168 ppt, accounting for 4.8% and 2.7% of the total $C_xH_yO_z$ and $C_xH_yO_zN_i$ concentrations (Fig. 2d and 2e). For $C_xH_yO_z$ category, the annual mean concentrations of species with 3, 4, 5, and ≥6 oxygens are 2352, 270, 21, and 7.4 ppt, respectively. For $C_xH_yO_zN_i$ category, the annual mean concentrations of species with 3, 4, 5, and ≥6 oxygens are 52, 18, 3.4, and 0.9 ppt, respectively. Organic vapors with 3 oxygens constitute the overwhelming majority of the concentration of measured organic vapors with more than three oxygens. As a result, the concentration weighted carbon number and DBE distributions (Fig. 3d and Fig. 3e) are significantly different from that of species number distributions for organic vapors with multiple oxygens. The concentrations of species with carbon numbers ranging from 2 to 6 are significantly higher, with those containing four carbons exhibiting the highest concentrations. Similarly, the concentrations of species with DBE ranging from 0-4 are notably higher than that of other DBE values. As compounds containing 3 oxygens dominate the concentration, IVOCs nearly entirely contribute to the concentration-weighted volatility of organic vapors with multiple oxygens (Fig. 3f). The concentrations of organic vapors with multiple oxygens measured in this study are higher than other studies, which will be detailed in Section 3.3.

Many of the measured organic vapors with multiple oxygens are multi-generation oxidants products of various VOC precursors in urban Beijing. Figure 4 displays the mass spectra of different carbon numbers from 2-11. Chemical formulas of the identified species with multiple oxygens are also summarized in Table S4. Take isoprene as an example, various oxidation products of isoprene are detected, including $C_5H_{10}O_3$ and subsequent oxidation products in C5 species, e.g., $C_5H_8O_6$, $C_5H_9NO_4$, etc. (Wennberg et al., 2018). For two additional important oxidation products of isoprene, methacrolein (MACR) and methyl vinyl ketone (MVK), their oxidation products are measured

https://doi.org/10.5194/egusphere-2024-1325
Preprint. Discussion started: 22 May 2024

in C4 species, such as $C_4H_7NO_4$, $C_4H_4O_3$, etc. Oxidation products of precursors such as benzene (C6) (Priestley et al., 2021), alkyl-substituted benzenes (C7-C9) (Pan and Wang, 2014; Wang et al., 2020c; Cheng et al., 2021), and monoterpenes (C10) (Rolletter et al., 2019) have also been determined. Besides, we can also detect some organic vapors with relatively low DBE (≤3), which may originate from the oxidation of aliphatic precursors. For example, $C_5H_8O_4$ are one of the oxidation products of C5 aldehyde, the photolysis of which release OH radicals, which may explain the missing source of OH radicals (Yang et al., 2024). Using Vocus-PTR can simultaneously measure precursors and multi-generational oxygenated products, which is beneficial for studying the evolution process of organic compounds in the atmosphere. Moreover, these organic vapors with multiple oxygens measured in this study may potentially supplement the "missing VOCs" when calculating OH reactivity, thereby improve the accuracy of diagnosis of sensitivity regimes for ozone formation (Wang et al., 2024). Assuming a rapid OH rate constant for these organic vapors (1×10^{-10} cm^3 $molecule^{-1}$ s^{-1}), the OH reactivity could reach as high as 7.2 s^{-1} annually on average, potentially accounting for half of the total missing OH reactivity.

The overall concentration of organic vapors with multiple oxygens is the highest in winter, followed by summer, spring and the lowest in autumn (Fig. 5a). The concentrations expressed in mean ± standard deviation (ppt ± ppt) are 2318 ± 564, 2496 ± 1003, 1919 ± 967, and 3396 ± 1085 for spring, summer, autumn, and winter, respectively. Compounds with different oxygens exhibit different seasonal variations, shown in Figure 5b and 5c and Table S3. For $C_xH_yO_z$ with 3 or 4 oxygens, the concentrations are higher in winter than in other seasons, while for compounds containing 5 or more oxygens, the concentrations are highest in summer. For $C_xH_yO_zN_i$ with 3 or 4 oxygens, the concentrations are high in both summer and winter, while for compounds containing 5 or more oxygens, the concentrations are high in summer and spring. As the oxygen number increases, the contribution from secondary sources becomes greater, and the high concentration of oxidants in summer intensifies this process. Thus, the fraction of the concentration of compounds with multiple oxygens increases with the oxygen number in summer (Fig. 5d). In winter, the concentrations of compounds containing five or more oxygens are significantly suppressed, which may be due to reduced generation. Alternatively, it could be that these compounds belong to SVOCs, with a majority being partitioned onto particulate matter at low temperatures.

The seasonal variations of organic vapors with multiple oxygens differ from those of total OVOCs (Fig. S5), with the latter's concentrations being primarily influenced by organic vapors containing 1-2 oxygen atoms. The concentration of total OVOCs in winter is significantly higher than in the other three seasons, followed by autumn and summer, with the lowest concentration observed in

https://doi.org/10.5194/egusphere-2024-1325
Preprint. Discussion started: 22 May 2024

spring. Cluster analysis is performed to further explore the dominated driving factors of the seasonal variations of organic vapors with multiple oxygens. Three clusters are identified in each season based on the diurnal profiles of each compound. To increase the interpretability of the clusters, two of them are merged. Figure 6 and Figure S6 shows the cluster results for organic vapors with multiple oxygens. For comparison, cluster analysis is performed on organic vapors with 1-2 oxygens as well (Fig. S7 and Fig. S8).

Daytime clusters, where the peak occurs during the daytime, were identified across the four seasons for organic vapors with multiple oxygens (shown as cluster 1 in Fig. 6). Daytime clusters for all seasons start to rise at 6:00, peak at noon and then slowly decrease, following the diurnal variation of solar radiation (Li et al., 2023) and ozone (Fig. S2), thereby suggesting that compounds in daytime clusters mainly originated from gas-phase photooxidation. Figure S9 also demonstrates the dependence of daytime clusters on temperature. The number and corresponding concentrations of species allocated to the daytime clusters vary in four seasons. In summer, the vast majority of species (75.1%) exhibit daytime characteristics, with a concentration percentage as high as 80.6%. The contribution of daytime clusters in autumn is also significant, with 66.5% and 59.3% of the species and concentrations being accounted for. The noon peaks of daytime clusters in winter and spring are relatively less pronounced, with the species and concentration day/night ratios also being comparatively lower. For organic vapors with 1 or 2 oxygens, a significant daytime cluster is observed only in summer (Fig. S7 d-f).

Another cluster type is considered to be nighttime clusters, as the corresponding species have their highest concentrations at night. Unlike the daytime cluster, the diurnal variations of nighttime clusters are different in four seasons (Fig. 6). In spring, the nighttime cluster comprises over 89.8% of nighttime species and 75.0% of concentrations, and it peaks at 4:00 with low daytime values. The nighttime clusters in winter and autumn show bimodal diurnal variations, with the highest peak occurring during the night from 19:00 to 23:00, and the second peak appearing during the day from 8:00 to 12:00. 60.4% and 33.5% of species exhibit the characteristics of the nighttime cluster in winter and autumn, constituting 64.9% and 40.7% of the mass concentration, respectively. The contribution of the nighttime cluster is minimal in summer, reaching its peak at midnight. We found that each nighttime cluster of organic vapors with multiple oxygens shows good consistency with the corresponding major clusters of organic vapors containing 1-2 oxygens (Fig. S7 and Fig. S10), while the concentrations during midday differ. Nighttime clusters have a similar origin to organic vapors containing 1-2 oxygens, mainly originating from primary emissions but are influenced by more secondary sources.

Most organic vapors with multiple oxygens could be assigned to different

https://doi.org/10.5194/egusphere-2024-1325
Preprint. Discussion started: 22 May 2024

clusters in different seasons (Fig. S11). Only a small number of species can be categorized into the same cluster in four seasons. Figure S12 shows the average C, H, O, and N number of species assigned to daytime cluster 0-4 times during the four seasons. As compounds exhibit more characteristics associated with daytime cluster, there is no significant change in the carbon number, but there is an increase in hydrogen and oxygen number, and a decrease in nitrogen number. This may be due to multi-step oxidation reactions in the atmosphere, causing an increase in oxygen number and DBE of species (Kroll et al., 2011; Isaacman-Vanwertz et al., 2018), with diurnal variations peaking at noon as a result of the strongest photochemistry. The decreasing trend of the number of nitrogen atoms in Figure S12 indicates that nitrogen containing compounds measured in this study are more likely to come from nocturnal production or emissions. Regarding the average elemental composition (C, H, O, and N) of species assigned to two clusters (see Fig. S13), daytime clusters typically exhibit higher oxygen content and lower H/C compared to nighttime clusters, providing further evidence supporting the atmospheric photochemical origin of daytime clusters. The nighttime clusters have higher nitrogen contents than daytime clusters, indicating more of the impacts of nocturnal sources.

3.3 Organic vapors with low oxygen content

In addition to multiple oxygens, organic vapors with low oxygen content are also measured in urban Beijing in this study. Here we primarily discuss comparisons between the results of this study and those of previous studies. The concentrations and variations of typical VOCs measured in this study are comparable to the results obtained by traditional PTR-MS measurements in both urban Beijing and neighboring regions. Figure S14 shows the diurnal profiles of 12 representative VOCs in four seasons. OVOCs of C_2H_4O, C_3H_6O, C_4H_8O, and C_4H_4O, usually identified as acetaldehyde, acetone, methyl ethyl ketone (MEK), and furan, are mainly from anthropogenic sources as reported by previous studies (Qian et al., 2019). Their diurnal variations exhibit a characteristic of being higher at night and lower during the day, similar to other studies reported in Beijing during the winter (Sheng et al., 2018; He et al., 2022). The concentrations of acetaldehyde, MEK and furan in winter are consistent with those observed in winter Beijing in 2016 and 2018 (Sheng et al., 2018; He et al., 2022). The winter concentrations of acetone are considerably higher than other seasons and observed in other studies, indicating an unknown strong emission source during the winter. The concentrations of benzene (C_6H_6), toluene (C_7H_8), and naphthalene ($C_{10}H_8$) in winter are slightly lower than reported in winter Beijing in the past few years (Sheng et al., 2018; Li et al., 2019; He et al., 2022), possibly due to improvements in air pollution policies, especially those targeting emissions from residential combustion and motor vehicles (Liu et al., 2023). As for phenols, the concentrations of C_6H_6O are

https://doi.org/10.5194/egusphere-2024-1325
Preprint. Discussion started: 22 May 2024

similar to measurement at a background site in the North China Plain in winter, while the concentrations of C_7H_8O are much lower than that (He et al., 2022). High concentrations of biogenic emissions in summer are overserved, for example isoprene (C_5H_8) and the sum of its oxidation products MACR and MVK (Apel et al., 2002) have daytime summer concentrations of 1.3 ppb and 0.7 ppb, respectively. Their concentrations in winter are lower and consistent with other studies (Sheng et al., 2018; He et al., 2022).

The mass fractions of organic categories in urban Beijing using Vocus-PTR differ from the results obtained using traditional PTR-MS. Previous studies in Beijing have only reported a few selected VOCs up to around 100 species, resulting in limited results on systematic characterizations of VOCs using PTR-MS in Beijing (Sheng et al., 2018; Li et al., 2019; Wang et al., 2021; Liu et al., 2022). Therefore, we compare with a suburban site, Gucheng, which is located 100 km southwest from our site. The two sites (urban Beijing and Gucheng) are both located in the North China Plain and are subject to regional air pollutions simultaneously. Figure S15 shows the comparison results of five categories, including C_xH_y, C_xH_yO, $C_xH_yO_2$, $C_xH_yO_{\geq 3}$, and N/S containing compounds. The first difference is that the mass fraction of species containing two or more oxygens measured by Vocus-PTR is higher than those measured by traditional PTR-MS. The mass fractions of $C_xH_yO_2$ and $C_xH_yO_{\geq 3}$ in Vocus-PTR are 20% and 5%, respectively, whereas they are 6% and 1% for traditional PTR-MS. In terms of concentrations, the concentration of $C_xH_yO_{\geq 3}$ is approximately double in Vocus-PTR, while the concentration of C_xH_yO is one-third compared to traditional PTR-MS measurement. The concentration of $C_xH_yO_2$ remains similar. This is because Vocus-PTR can detect more OVOCs with multiple oxygens due to its high sensitivity and mass resolution, whereas due to its low transmission efficiency for low masses, it is difficult to detect high concentration OVOCs such as methanol and formaldehyde. The other difference is that the mass fraction and concentration of C_xH_y species measured by Vocus-PTR are much lower than those measured by traditional PTR. For several major C_xH_y compounds such as benzene, C7, C8, and C9 aromatics, their concentrations are comparable between the two methods. The main difference between the two methods lies in the concentration of low-mass hydrocarbons. Overall, when applied to the urban atmosphere, Vocus-PTR has advantages in measuring oxygenated VOCs, especially with multiple oxygens. However, it has limitations in measuring low molecular weight VOCs due to the low-mass cutoff in the transmission efficiency.

The molecular characteristics of organic vapors measured by Vocus-PTR in urban Beijing show several differences from those in forested areas (Li et al., 2020; Huang et al., 2021; Li et al., 2021). Firstly, organics up to 300 m/z can be observed in forested areas, while organics up to 230 m/z are observed (Fig. 1a). Two main reasons are responsible for this. The complexity of the species

https://doi.org/10.5194/egusphere-2024-1325
Preprint. Discussion started: 22 May 2024

introduces challenges in interpreting mass spectra, which is evidenced by the total number of species being similar to existing atmospheric measurements using Vocus-PTR, despite a narrower mass range in this study. The higher particulate matter concentrations in urban area provide a larger sink for organic vapors (Deng et al., 2020), and this loss effect is especially pronounced for compounds with high molecular weights due to their lower volatility. The second difference is that, $C_xH_yO_z$ and $C_xH_yO_zN_i$ species are the dominant main organics in both urban and forested areas, whilst $C_xH_yN_i$ species are more common and abundant in urban area, which may come from biomass burning emissions (Laskin et al., 2009). Thirdly, VOCs with low carbon and oxygen number play a more significant role in total organic concentration compared to results from forested regions. As shown in Figure S16a, C_2 and C_3 organics contribute 77% of the total organic concentration in this study, while C_4-C_6 organics contribute approximately 75% in forested regions. In contrast to forested areas, where VOCs and IVOCs concentrations are comparable, the majority of the total organic concentration is attributed to VOCs in this study (Fig. S16b). Typical C_2 and C_3 organics, such as C_3H_6O, $C_2H_4O_2$, and C_2H_4O, contribute 18%, 12%, and 11%, respectively, to the total organic concentration, which are mainly originated from anthropogenic emissions including industrial and vehicular activities, solvent utilization, and other sources (Qian et al., 2019).

4 Conclusions

In this study, we explore the molecular and seasonal characteristics of organic vapors in urban Beijing using a Vocus-PTR over four seasons. A total of 895 peaks are observed, and 543 of them can be assigned to formulas. The contribution of $C_xH_yO_z$ species is most significant, which compose up to 53.7% of the number and 76.0% of the concentrations of total organics. With enhanced sensitivity and mass resolution, an increased number of species have been discovered compared to traditional PTR-MS measurements in urban Beijing, especially compounds with lower concentrations and higher oxygen contents. 42.2% species in number measured in this study are at sub-ppt level and 37.8% species in number contain 3-8 oxygens, resulting in a higher fraction of species containing three or more oxygens compared to traditional PTR-MS measurements. The molecular characteristics of VOCs in urban area show differences with current Vocus-PTR measurements in forested areas. $C_xH_yO_z$ and $C_xH_yO_zN_i$ species are the main organics in both urban and forested areas, whilst $C_xH_yN_i$ species are more ubiquitous and abundant in urban area, originating from anthropogenic emissions. Organic vapors with low carbon and oxygen content exert a more substantial influence on the overall organic concentration in urban Beijing than in forested areas. Organic vapors with low oxygen content are effectively measured in this study and are comparable to those obtained in both urban Beijing and neighboring regions. Organic vapors

https://doi.org/10.5194/egusphere-2024-1325
Preprint. Discussion started: 22 May 2024

with multiple oxygens are mainly IVOCs and SVOCs. The overall concentration of organic vapors with multiple oxygens is highest in winter, followed by summer, spring and lowest in autumn. As the oxygen number increases, the impact of the photooxidation process becomes more pronounced, leading to an increase in both concentration and proportion of organic vapors with multiple oxygens during the summer season. Combining the cluster analysis, we identify daytime clusters (peaking at noon) for organic vapors with multiple oxygens in all seasons, which is distinct from organic vapors with one or two oxygens. In summer, the majority of species are aligned to daytime cluster, primarily originating from the photooxidation process. We also found that nighttime clusters (peaking at night) show good consistency with the cluster of organic vapors with one or two oxygens. In spring and winter when the nighttime cluster dominated, the variations of organic vapors with multiple oxygens are strongly correlated with organic vapors with one or two oxygens.

The measured compositions and seasonal variabilities of organic vapors with multiple oxygens emphasize the importance of high sensitivity and high mass resolution measurement in urban atmosphere. These organics with multiple oxygens could both supplement missed OH reactivity and contribute to secondary organic aerosol formation due to their low volatility, suggesting prospective for future research.

https://doi.org/10.5194/egusphere-2024-1325
Preprint. Discussion started: 22 May 2024

Figures

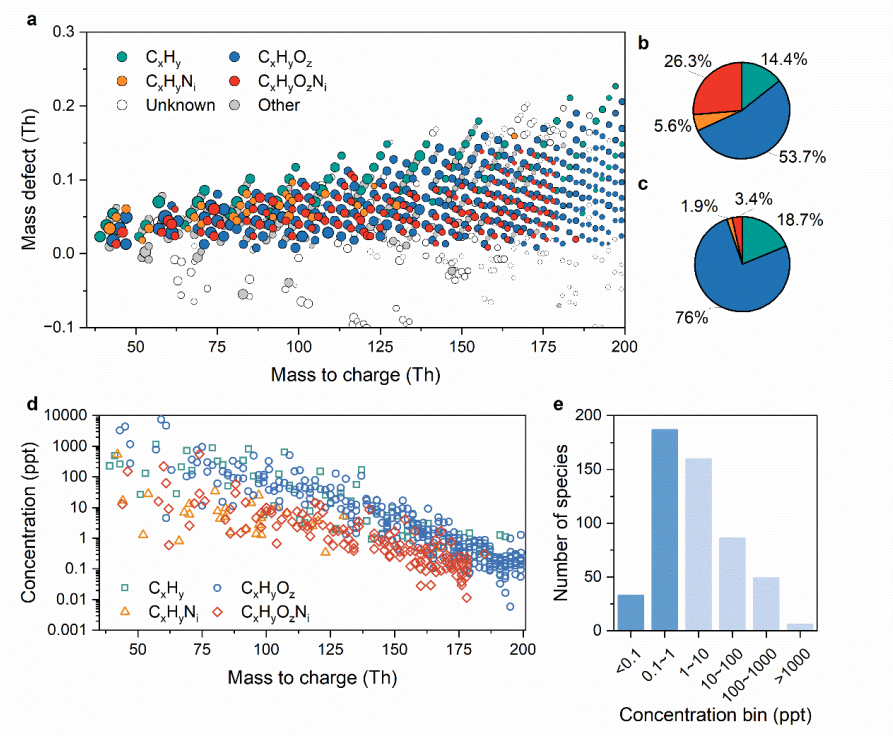

Figure 1. Identified organics in urban Beijing using Vocus-PTR. (a) Mass defect plot. The sizes of the bubbles represent the annual median concentrations. The bubbles are colored by different elemental compositions as labeled in the legend. The "unknown" refers to fitted peaks without matched formula. The "other" refers to compounds containing elements other than C, H, O, and N or fragment peaks (or radicals). (b) Pie chart of the number of organic vapors. (c) Pie chart of the annual median concentrations of organic vapors. The colors of the pie charts are consistent with the mass defect plot. (d) The annual median concentrations of organic vapors versus their masses. (e) Histogram of annual concentrations of organic vapors. Bins with values less than 1 ppt are emphasized in dark color.

https://doi.org/10.5194/egusphere-2024-1325
Preprint. Discussion started: 22 May 2024

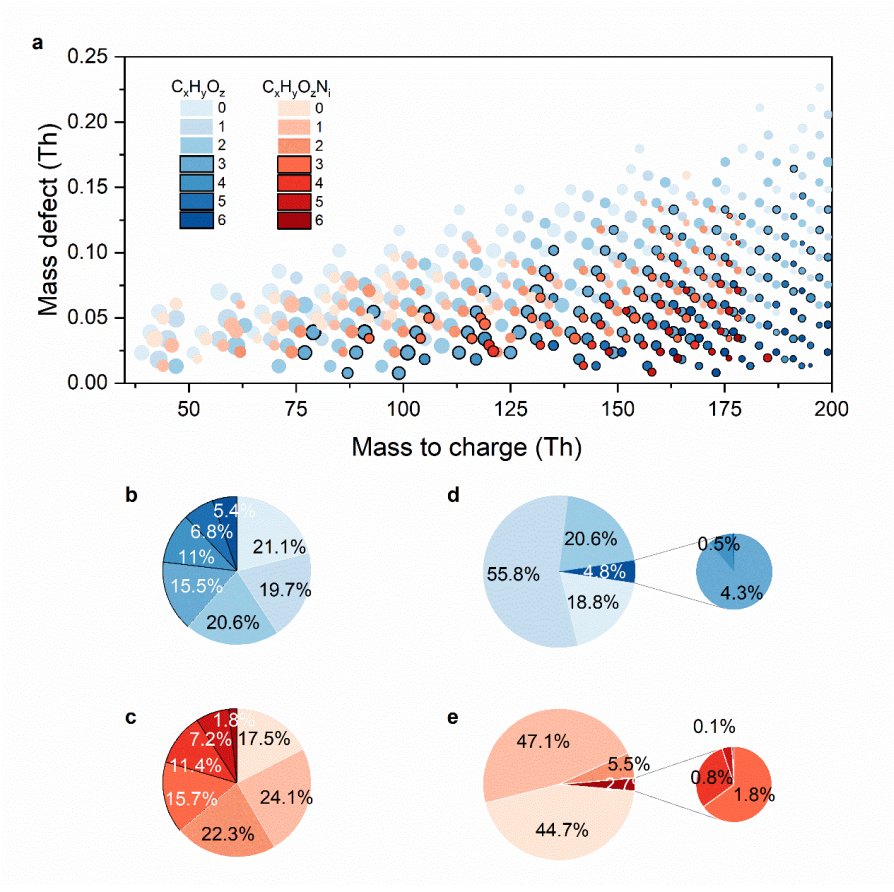

Figure 2. Organic vapors of different oxygen content. (a) Mass defect plot. The sizes of the bubbles are determined by the annual median concentrations. The bubbles are colored by different oxygen numbers as labeled in the legend. Bars labeled as 6 refers to organic vapors with oxygen number equal or larger than 6. Bubbles representing organic vapors with 3 or more oxygens are highlighted with black borders. (b) Pie chart of the number of $C_xH_yO_z$ species. (c) Pie chart of the number of $C_xH_yO_zN_i$ species. (d) Pie chart of the concentration of $C_xH_yO_z$ species. (e) Pie chart of the concentration of $C_xH_yO_zN_i$ species. The color of the pie charts is consistent with the mass defect plot.

https://doi.org/10.5194/egusphere-2024-1325
Preprint. Discussion started: 22 May 2024

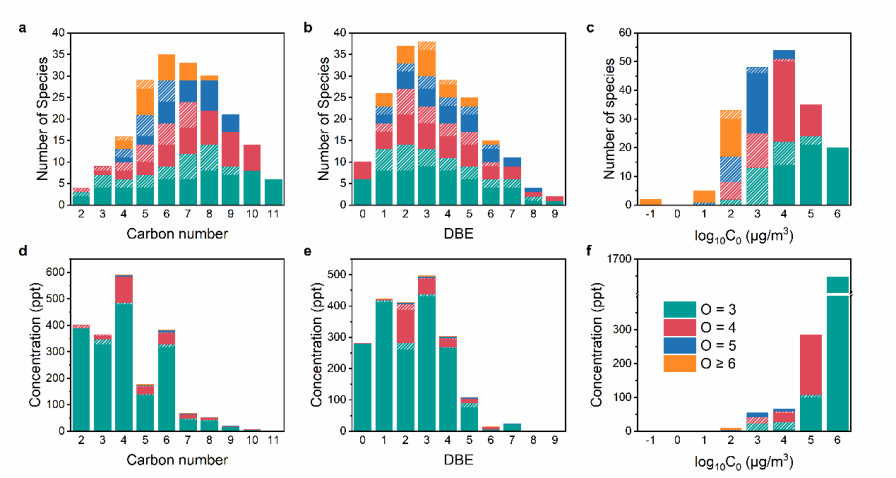

Figure 3. Distribution of carbon number, double bond equivalent (DBE), and volatility of organic vapors with multiple oxygens. Panels (a) - (c) represent species number distributions of carbon number, DBE, and volatility, respectively. Panels (d) - (e) represent concentration distributions of carbon number, DBE, and volatility, respectively. Different color of bars refers to compounds with different oxygens. Bars without white stripes represent $C_xH_yO_{\geq 3}$, while shaded bars with white stripes represent $C_xH_yO_{\geq 3}N$. Y axials refer to annual median concentrations.

https://doi.org/10.5194/egusphere-2024-1325
Preprint. Discussion started: 22 May 2024

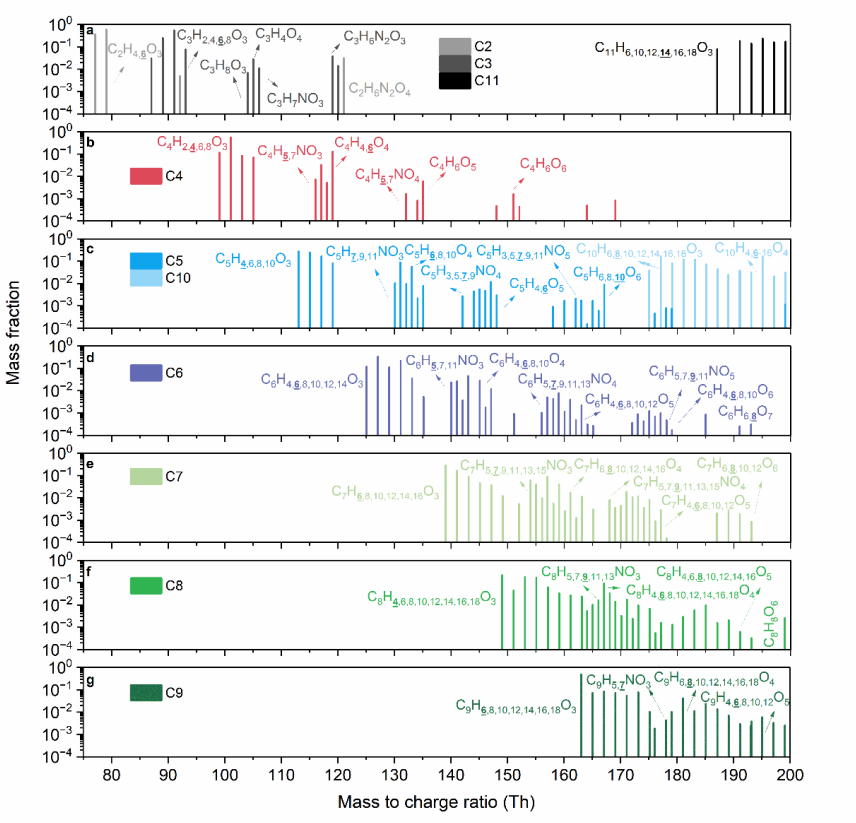

Figure 4. Mass spectra of organic vapors with multiple oxygens with different carbon numbers. The y axis shows the annual median mass fraction of organic vapors for each carbon number, which means that for different organic vapors with the same carbon number, the sum of the mass fractions equals 1. The formula of organics vapors with multiple oxygens are labelled. In molecular formulas with the same number of carbons and oxygens, the hydrogen content in the organic vapors with the highest intensity is emphasized by bold and underlined formatting. (a) C2, C3, and C11. (b) C4. (c) C5 and C10. (d) C6. (e) C7. (f) C8. (g) C9.

https://doi.org/10.5194/egusphere-2024-1325
Preprint. Discussion started: 22 May 2024

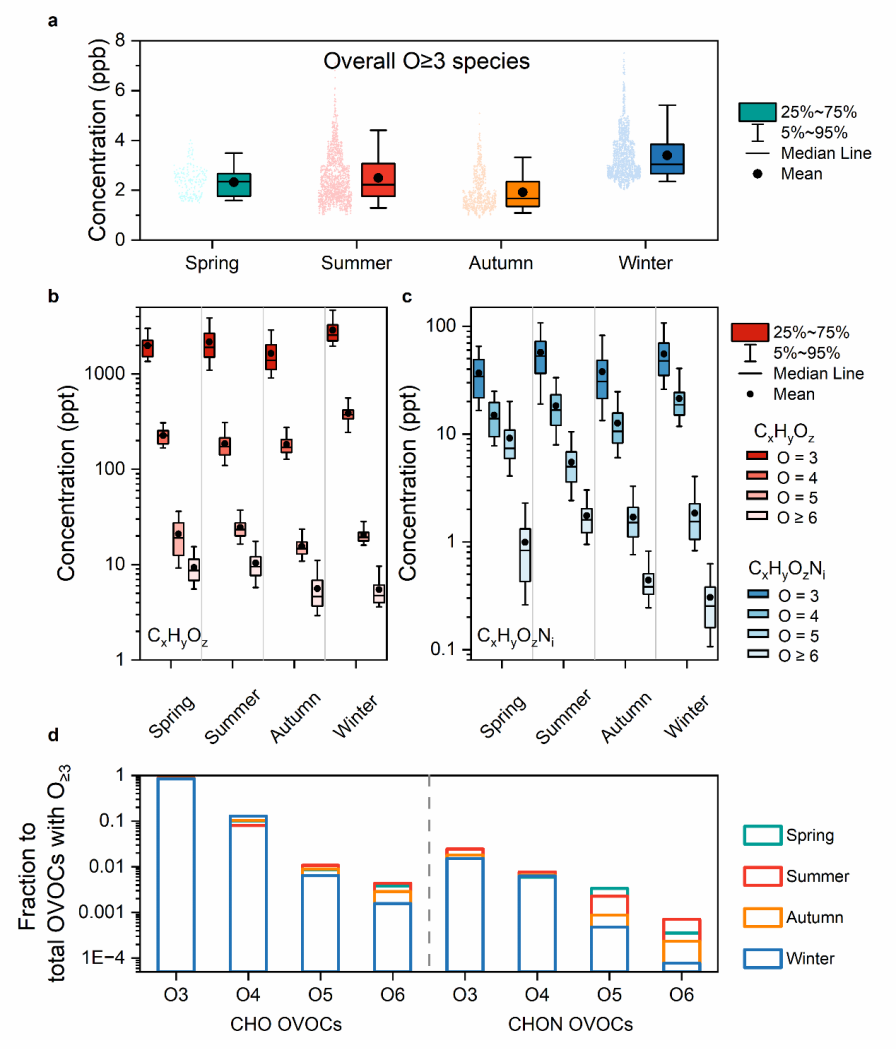

Figure 5. Seasonal variations of organic vapors with multiple oxygens in urban Beijing. (a) Total organic vapors with multiple oxygens. (b) $C_xH_yO_z$ with different oxygens. (c) $C_xH_yO_zN_i$ with different oxygens. (d) Fractions of organic vapors with different oxygens to total organic vapors with multiple oxygens.

https://doi.org/10.5194/egusphere-2024-1325
Preprint. Discussion started: 22 May 2024

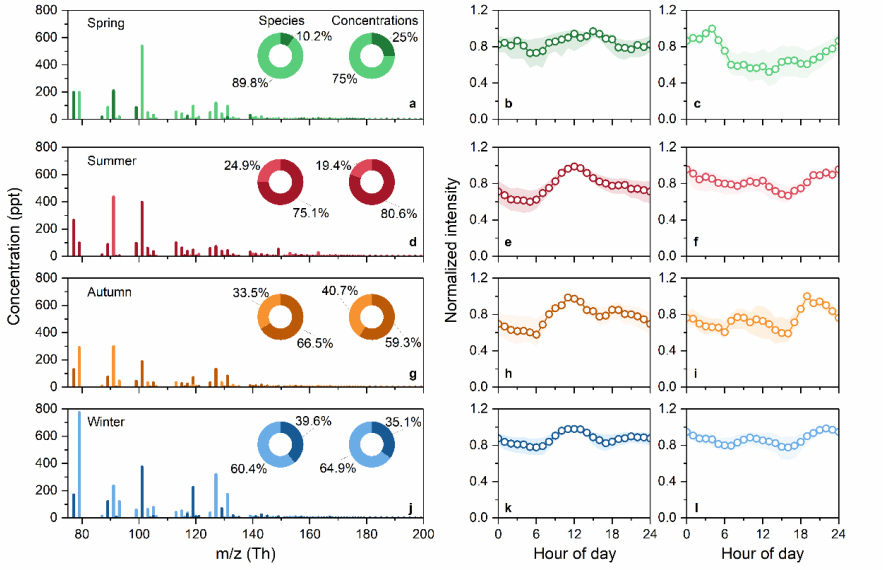

Figure 6. Cluster results of organic vapors with multiple oxygens in four seasons. (a) – (c) Cluster results for spring. (a) Mass spectra of organic vapors with multiple oxygens in spring. Y axis is the median concentration of each compound. Two different shades of colors are used to distinguish between two clusters. Two pie charts represent the distribution of species numbers and concentrations of organic vapors for two clusters. (b) Normalized median diurnal variation of cluster 1, daytime cluster. (c) Normalized median diurnal variation of cluster 2, nighttime cluster. The shaded areas in the graph (b) and (c) represent the 25th and 75th percentiles. (d) – (f) Cluster results for summer. (g) to (i) Cluster results for autumn. (j) – (l) Cluster results for winter.

https://doi.org/10.5194/egusphere-2024-1325
Preprint. Discussion started: 22 May 2024

Data availability

Data are available upon request from the corresponding author.

Supplement

The content of the Supplement includes the map of the observation site (Fig. S1); the diurnal variations of $PM_{2.5}$, O_3, NO_x, RH, and T in four seasons (Fig. S2); calibration results of mixed calibration gases (Fig. S3); carbon oxidation state of organic vapors with different oxygens (Fig. S4); boxplot of total OVOC concentrations in four seasons (Fig. S5); diurnal variation cluster results of organic vapors with multiple oxygens (Fig. S6); cluster results of organic vapors with one or two oxygens (Fig. S7-S8); dependence of daytime clusters on temperature (Fig. S9); dependence of nighttime clusters on major clusters of organic vapors with 1-2 oxygens (Fig. S10); the distribution of organic vapors with multiple oxygens across different clusters (Fig. S11); average C, H, O, and N number of organic vapors containing multiple oxygens with different diurnal patterns (Fig. S12); average C, H, O, and N number of organic vapors containing multiple oxygens in two clusters (Fig. S13); diurnal profiles of representative VOCs in four seasons (Fig. S14); comparison results with Gucheng site (Fig. S15); molecular characteristics of total measured organic vapors by Vocus-PTR (Fig. S16); the observation periods of Vocus-PTR (Table S1); information about calibration gases (Table S2); seasonal concentrations of OVOCs with multiple oxygens (Table S3); and main $C_xH_yO_{\geq 3}$ and $C_xH_yO_{\geq 3}N$ species measured in this study (Table S4).

Author contributions

Conceptualization: JJ and ZA. Data collection and analysis: ZA, RY, XZ, XxL, YY, JG, YuL, and XuL. Writing-original draft: ZA. Writing-review and editing: XxL, DL, YaL, DW, CY, KH, DRW, FNK, and JJ.

Competing interests

At least one of the (co-)authors is a member of the editorial board of *Atmospheric Chemistry and Physics*.

Financial support

This work has been supported by the National Natural Science Foundation of China (Grant NO. 22206097, 22188102, and 22106083) and Samsung $PM_{2.5}$ SRP.

https://doi.org/10.5194/egusphere-2024-1325
Preprint. Discussion started: 22 May 2024

References

Apel, E. C., Riemer, D. D., Hills, A., Baugh, W., Orlando, J., Faloona, I., Tan, D., Brune, W., Lamb, B., Westberg, H., Carroll, M. A., Thornberry, T., and Geron, C. D.: Measurement and interpretation of isoprene fluxes and isoprene, methacrolein, and methyl vinyl ketone mixing ratios at the PROPHET site during the 1998 Intensive, J. Geophys. Res.: Atmos., 107, 10.1029/2000jd000225, 2002.

Breitenlechner, M., Fischer, L., Hainer, M., Heinritzi, M., Curtius, J., and Hansel, A.: PTR3: An Instrument for Studying the Lifecycle of Reactive Organic Carbon in the Atmosphere, Anal Chem, 89, 5824-5831, 10.1021/acs.analchem.6b05110, 2017.

Cai, R. and Jiang, J.: A new balance formula to estimate new particle formation rate: reevaluating the effect of coagulation scavenging, Atmos. Chem. Phys., 17, 12659-12675, 10.5194/acp-17-12659-2017, 2017.

Cappellin, L., Karl, T., Probst, M., Ismailova, O., Winkler, P. M., Soukoulis, C., Aprea, E., Mark, T. D., Gasperi, F., and Biasioli, F.: On quantitative determination of volatile organic compound concentrations using proton transfer reaction time-of-flight mass spectrometry, Environ Sci Technol, 46, 2283-2290, 10.1021/es203985t, 2012.

Carter, W. P. L.: Development of Ozone Reactivity Scales for Volatile Organic Compounds, Air & Waste, 44, 881-899, 10.1080/1073161X.1994.10467290, 1994.

Chang, Y., Wang, H., Gao, Y., Jing, S., Lu, Y., Lou, S., Kuang, Y., Cheng, K., Ling, Q., Zhu, L., Tan, W., and Huang, R. J.: Nonagricultural emissions dominate urban atmospheric amines as revealed by mobile measurements, Geophys. Res. Lett., 10.1029/2021gl097640, 2022.

Cheng, X., Chen, Q., Jie Li, Y., Zheng, Y., Liao, K., and Huang, G.: Highly oxygenated organic molecules produced by the oxidation of benzene and toluene in a wide range of OH exposure and NOx conditions, Atmos. Chem. Phys., 21, 12005-12019, 10.5194/acp-21-12005-2021, 2021.

de Gouw, J. and Warneke, C.: Measurements of volatile organic compounds in the earth's atmosphere using proton-transfer-reaction mass spectrometry, Mass Spectrom Rev, 26, 223-257, 10.1002/mas.20119, 2007.

Deng, C., Fu, Y., Dada, L., Yan, C., Cai, R., Yang, D., Zhou, Y., Yin, R., Lu, Y., Li, X., Qiao, X., Fan, X., Nie, W., Kontkanen, J., Kangasluoma, J., Chu, B., Ding, A., Kerminen, V. M., Paasonen, P., Worsnop, D. R., Bianchi, F., Liu, Y., Zheng, J., Wang, L., Kulmala, M., and Jiang, J.: Seasonal Characteristics of New Particle Formation and Growth in Urban Beijing, Environ Sci Technol, 54, 8547-8557, 10.1021/acs.est.0c00808, 2020.

Fischer, L., Breitenlechner, M., Canaval, E., Scholz, W., Striednig, M., Graus, M., Karl, T. G., Petäjä, T., Kulmala, M., and Hansel, A.: First eddy covariance flux measurements of semi-volatile organic compounds with the PTR3-TOF-MS, Atmos. Meas. Tech., 14, 8019-8039, 10.5194/amt-14-8019-2021, 2021.

Gentner, D. R., Worton, D. R., Isaacman, G., Davis, L. C., Dallmann, T. R., Wood, E. C., Herndon, S. C., Goldstein, A. H., and Harley, R. A.: Chemical Composition of Gas-Phase Organic Carbon Emissions from Motor Vehicles and Implications for Ozone Production, Environ. Sci. Technol., 47, 11837-11848, 10.1021/es401470e, 2013.

https://doi.org/10.5194/egusphere-2024-1325
Preprint. Discussion started: 22 May 2024

Gilman, J. B., Lerner, B. M., Kuster, W. C., Goldan, P. D., Warneke, C., Veres, P. R., Roberts, J. M., de Gouw, J. A., Burling, I. R., and Yokelson, R. J.: Biomass burning emissions and potential air quality impacts of volatile organic compounds and other trace gases from fuels common in the US, Atmos. Chem. Phys., 15, 13915-13938, 10.5194/acp-15-13915-2015, 2015.

Goldstein, A. H. and Galbally, I. E.: Known and Unexplored Organic Constituents in the Earth's Atmosphere, Environ. Sci. Technol., 41, 1514-1521, 10.1021/es072476p, 2007.

Graus, M., Müller, M., and Hansel, A.: High resolution PTR-TOF: Quantification and formula confirmation of VOC in real time, J. Am. Soc. Mass Spectrom., 21, 1037-1044, 10.1016/j.jasms.2010.02.006, 2010.

Hallquist, M., Wenger, J. C., Baltensperger, U., Rudich, Y., Simpson, D., Claeys, M., Dommen, J., Donahue, N. M., George, C., Goldstein, A. H., Hamilton, J. F., Herrmann, H., Hoffmann, T., Iinuma, Y., Jang, M., Jenkin, M. E., Jimenez, J. L., Kiendler-Scharr, A., Maenhaut, W., McFiggans, G., Mentel, T. F., Monod, A., Prévôt, A. S. H., Seinfeld, J. H., Surratt, J. D., Szmigielski, R., and Wildt, J.: The formation, properties and impact of secondary organic aerosol: current and emerging issues, Atmos. Chem. Phys., 9, 5155-5236, 10.5194/acp-9-5155-2009, 2009.

Hansel, A., Jordan, A., Holzinger, R., Prazeller, P., Vogel, W., and Lindinger, W.: Proton transfer reaction mass spectrometry: on-line trace gas analysis at the ppb level, International Journal of Mass Spectrometry and Ion Processes, 149-150, 609-619, https://doi.org/10.1016/0168-1176(95)04294-U, 1995.

He, X., Yuan, B., Wu, C., Wang, S., Wang, C., Huangfu, Y., Qi, J., Ma, N., Xu, W., Wang, M., Chen, W., Su, H., Cheng, Y., and Shao, M.: Volatile organic compounds in wintertime North China Plain: Insights from measurements of proton transfer reaction time-of-flight mass spectrometer (PTR-ToF-MS), Journal of Environmental Sciences, 10.1016/j.jes.2021.08.010, 2022.

Huang, W., Li, H., Sarnela, N., Heikkinen, L., Tham, Y. J., Mikkilä, J., Thomas, S. J., Donahue, N. M., Kulmala, M., and Bianchi, F.: Measurement report: Molecular composition and volatility of gaseous organic compounds in a boreal forest – from volatile organic compounds to highly oxygenated organic molecules, Atmos. Chem. Phys., 21, 8961-8977, 10.5194/acp-21-8961-2021, 2021.

Isaacman-VanWertz, G., Massoli, P., O'Brien, R., Lim, C., Franklin, J. P., Moss, J. A., Hunter, J. F., Nowak, J. B., Canagaratna, M. R., Misztal, P. K., Arata, C., Roscioli, J. R., Herndon, S. T., Onasch, T. B., Lambe, A. T., Jayne, J. T., Su, L., Knopf, D. A., Goldstein, A. H., Worsnop, D. R., and Kroll, J. H.: Chemical evolution of atmospheric organic carbon over multiple generations of oxidation, Nat Chem, 10, 462-468, 10.1038/s41557-018-0002-2, 2018.

Jahn, L. G., Tang, M., Blomdahl, D., Bhattacharyya, N., Abue, P., Novoselac, A., Ruiz, L. H., and Misztal, P. K.: Volatile organic compound (VOC) emissions from the usage of benzalkonium chloride and other disinfectants based on quaternary ammonium compounds, Environmental Science: Atmospheres, 3, 363-373, 10.1039/d2ea00054g, 2023.

Jensen, A. R., Koss, A. R., Hales, R. B., and de Gouw, J. A.: Measurements of volatile organic compounds in ambient air by gas-chromatography and real-time Vocus PTR-TOF-MS: calibrations, instrument background corrections, and introducing a PTR Data Toolkit, Atmos. Meas. Tech., 16, 5261-5285, 10.5194/amt-16-5261-2023, 2023.

Jimenez, J. L., Canagaratna, M. R., Donahue, N. M., Prevot, A. S. H., Zhang,

https://doi.org/10.5194/egusphere-2024-1325
Preprint. Discussion started: 22 May 2024

764 Q., Kroll, J. H., DeCarlo, P. F., Allan, J. D., Coe, H., Ng, N. L., Aiken, A. C.,
765 Docherty, K. S., Ulbrich, I. M., Grieshop, A. P., Robinson, A. L., Duplissy, J.,
766 Smith, J. D., Wilson, K. R., Lanz, V. A., Hueglin, C., Sun, Y. L., Tian, J.,
767 Laaksonen, A., Raatikainen, T., Rautiainen, J., Vaattovaara, P., Ehn, M.,
768 Kulmala, M., Tomlinson, J. M., Collins, D. R., Cubison, M. J., Dunlea, E. J.,
769 Huffman, J. A., Onasch, T. B., Alfarra, M. R., Williams, P. I., Bower, K., Kondo,
770 Y., Schneider, J., Drewnick, F., Borrmann, S., Weimer, S., Demerjian, K.,
771 Salcedo, D., Cottrell, L., Griffin, R., Takami, A., Miyoshi, T., Hatakeyama, S.,
772 Shimono, A., Sun, J. Y., Zhang, Y. M., Dzepina, K., Kimmel, J. R., Sueper, D.,
773 Jayne, J. T., Herndon, S. C., Trimborn, A. M., Williams, L. R., Wood, E. C.,
774 Middlebrook, A. M., Kolb, C. E., Baltensperger, U., and Worsnop, D. R.:
775 Evolution of Organic Aerosols in the Atmosphere, Science, 326, 1525-1529,
776 10.1126/science.1180353, 2009.

777 Jordan, A., Haidacher, S., Hanel, G., Hartungen, E., Märk, L., Seehauser, H.,
778 Schottkowsky, R., Sulzer, P., and Märk, T. D.: A high resolution and high
779 sensitivity proton-transfer-reaction time-of-flight mass spectrometer (PTR-TOF-
780 MS), Int. J. Mass Spectrom., 286, 122-128,
781 https://doi.org/10.1016/j.ijms.2009.07.005, 2009.

782 Krechmer, J., Lopez-Hilfiker, F., Koss, A., Hutterli, M., Stoermer, C., Deming, B.,
783 Kimmel, J., Warneke, C., Holzinger, R., Jayne, J., Worsnop, D., Fuhrer, K.,
784 Gonin, M., and de Gouw, J.: Evaluation of a New Reagent-Ion Source and
785 Focusing Ion-Molecule Reactor for Use in Proton-Transfer-Reaction Mass
786 Spectrometry, Anal Chem, 90, 12011-12018, 10.1021/acs.analchem.8b02641,
787 2018.

788 Kroll, J. H., Donahue, N. M., Jimenez, J. L., Kessler, S. H., Canagaratna, M. R.,
789 Wilson, K. R., Altieri, K. E., Mazzoleni, L. R., Wozniak, A. S., Bluhm, H., Mysak,
790 E. R., Smith, J. D., Kolb, C. E., and Worsnop, D. R.: Carbon oxidation state as
791 a metric for describing the chemistry of atmospheric organic aerosol, Nature
792 Chemistry, 3, 133-139, 10.1038/nchem.948, 2011.

793 Laskin, A., Smith, J. S., and Laskin, J.: Molecular Characterization of Nitrogen-
794 Containing Organic Compounds in Biomass Burning Aerosols Using High-
795 Resolution Mass Spectrometry, Environ. Sci. Technol., 43, 3764-3771,
796 10.1021/es803456n, 2009.

797 Lewis, A. C., Carslaw, N., Marriott, P. J., Kinghorn, R. M., Morrison, P., Lee, A.
798 L., Bartle, K. D., and Pilling, M. J.: A larger pool of ozone-forming carbon
799 compounds in urban atmospheres, Nature, 405, 778-781, 2000.

800 Li, H., Almeida, T. G., Luo, Y., Zhao, J., Palm, B. B., Daub, C. D., Huang, W.,
801 Mohr, C., Krechmer, J. E., Kurtén, T., and Ehn, M.: Fragmentation inside proton-
802 transfer-reaction-based mass spectrometers limits the detection of ROOR and
803 ROOH peroxides, Atmos. Meas. Tech., 15, 1811-1827, 10.5194/amt-15-1811-
804 2022, 2022a.

805 Li, H., Riva, M., Rantala, P., Heikkinen, L., Daellenbach, K., Krechmer, J. E.,
806 Flaud, P.-M., Worsnop, D., Kulmala, M., Villenave, E., Perraudin, E., Ehn, M.,
807 and Bianchi, F.: Terpenes and their oxidation products in the French Landes
808 forest: insights from Vocus PTR-TOF measurements, Atmos. Chem. Phys., 20,
809 1941-1959, 10.5194/acp-20-1941-2020, 2020.

810 Li, H., Canagaratna, M. R., Riva, M., Rantala, P., Zhang, Y., Thomas, S.,
811 Heikkinen, L., Flaud, P.-M., Villenave, E., Perraudin, E., Worsnop, D., Kulmala,
812 M., Ehn, M., and Bianchi, F.: Atmospheric organic vapors in two European pine
813 forests measured by a Vocus PTR-TOF: insights into monoterpene and
814 sesquiterpene oxidation processes, Atmos. Chem. Phys., 21, 4123-4147,
815 10.5194/acp-21-4123-2021, 2021.

https://doi.org/10.5194/egusphere-2024-1325
Preprint. Discussion started: 22 May 2024

Li, K., Li, J., Tong, S., Wang, W., Huang, R.-J., and Ge, M.: Characteristics of wintertime VOCs in suburban and urban Beijing: concentrations, emission ratios, and festival effects, Atmos. Chem. Phys., 19, 8021-8036, 10.5194/acp-19-8021-2019, 2019.

Li, K., Zhang, J., Bell, D. M., Wang, T., Lamkaddam, H., Cui, T., Qi, L., Surdu, M., Wang, D., Du, L., El Haddad, I., Slowik, J. G., and Prevot, A. S. H.: Uncovering the dominant contribution of intermediate volatility compounds in secondary organic aerosol formation from biomass-burning emissions, Natl Sci Rev, 11, nwae014, 10.1093/nsr/nwae014, 2024.

Li, X.-B., Yuan, B., Wang, S., Wang, C., Lan, J., Liu, Z., Song, Y., He, X., Huangfu, Y., Pei, C., Cheng, P., Yang, S., Qi, J., Wu, C., Huang, S., You, Y., Chang, M., Zheng, H., Yang, W., Wang, X., and Shao, M.: Variations and sources of volatile organic compounds (VOCs) in urban region: insights from measurements on a tall tower, Atmos. Chem. Phys., 22, 10567-10587, 10.5194/acp-22-10567-2022, 2022b.

Li, X., Chen, Y., Li, Y., Cai, R., Li, Y., Deng, C., Wu, J., Yan, C., Cheng, H., Liu, Y., Kulmala, M., Hao, J., Smith, J. N., and Jiang, J.: Seasonal variations in composition and sources of atmospheric ultrafine particles in urban Beijing based on near-continuous measurements, Atmos. Chem. Phys., 23, 14801-14812, 10.5194/acp-23-14801-2023, 2023.

Li, Y., Pöschl, U., and Shiraiwa, M.: Molecular corridors and parameterizations of volatility in the chemical evolution of organic aerosols, Atmos. Chem. Phys., 16, 3327-3344, 10.5194/acp-16-3327-2016, 2016.

Liu, Q., Sheng, J., Wu, Y., Ma, Z., Sun, J., Tian, P., Zhao, D., Li, X., Hu, K., Li, S., Shen, X., Zhang, Y., He, H., Huang, M., Ding, D., and Liu, D.: Source characterization of volatile organic compounds in urban Beijing and its links to secondary organic aerosol formation, Sci. Total Environ., 10.1016/j.scitotenv.2022.160469, 2022.

Liu, Y., Yin, S., Zhang, S., Ma, W., Zhang, X., Qiu, P., Li, C., Wang, G., Hou, D., Zhang, X., An, J., Sun, Y., Li, J., Zhang, Z., Chen, J., Tian, H., Liu, X., and Liu, L.: Drivers and impacts of decreasing concentrations of atmospheric volatile organic compounds (VOCs) in Beijing during 2016-2020, Sci Total Environ, 906, 167847, 10.1016/j.scitotenv.2023.167847, 2023.

Millet, D. B., Baasandorj, M., Farmer, D. K., Thornton, J. A., Baumann, K., Brophy, P., Chaliyakunnel, S., de Gouw, J. A., Graus, M., Hu, L., Koss, A., Lee, B. H., Lopez-Hilfiker, F. D., Neuman, J. A., Paulot, F., Peischl, J., Pollack, I. B., Ryerson, T. B., Warneke, C., Williams, B. J., and Xu, J.: A large and ubiquitous source of atmospheric formic acid, Atmos. Chem. Phys., 15, 6283-6304, 10.5194/acp-15-6283-2015, 2015.

Noziere, B., Kalberer, M., Claeys, M., Allan, J., D'Anna, B., Decesari, S., Finessi, E., Glasius, M., Grgic, I., Hamilton, J. F., Hoffmann, T., Iinuma, Y., Jaoui, M., Kahnt, A., Kampf, C. J., Kourtchev, I., Maenhaut, W., Marsden, N., Saarikoski, S., Schnelle-Kreis, J., Surratt, J. D., Szidat, S., Szmigielski, R., and Wisthaler, A.: The molecular identification of organic compounds in the atmosphere: state of the art and challenges, Chemical Reviews, 115, 3919-3983, 10.1021/cr5003485, 2015.

Pan, S. and Wang, L.: Atmospheric oxidation mechanism of m-xylene initiated by OH radical, J Phys Chem A, 118, 10778-10787, 10.1021/jp506815v, 2014.

Priestley, M., Bannan, T. J., Le Breton, M., Worrall, S. D., Kang, S., Pullinen, I., Schmitt, S., Tillmann, R., Kleist, E., Zhao, D., Wildt, J., Garmash, O., Mehra, A., Bacak, A., Shallcross, D. E., Kiendler-Scharr, A., Hallquist, Å. M., Ehn, M., Coe,

https://doi.org/10.5194/egusphere-2024-1325
Preprint. Discussion started: 22 May 2024

H., Percival, C. J., Hallquist, M., Mentel, T. F., and McFiggans, G.: Chemical characterisation of benzene oxidation products under high- and low-NOx conditions using chemical ionisation mass spectrometry, Atmos. Chem. Phys., 21, 3473-3490, 10.5194/acp-21-3473-2021, 2021.

Pugliese, G., Ingrisch, J., Meredith, L. K., Pfannerstill, E. Y., Klupfel, T., Meeran, K., Byron, J., Purser, G., Gil-Loaiza, J., van Haren, J., Dontsova, K., Kreuzwieser, J., Ladd, S. N., Werner, C., and Williams, J.: Effects of drought and recovery on soil volatile organic compound fluxes in an experimental rainforest, Nat Commun, 14, 5064, 10.1038/s41467-023-40661-8, 2023.

Qian, X., Shen, H., and Chen, Z.: Characterizing summer and winter carbonyl compounds in Beijing atmosphere, Atmos. Environ., 214, 10.1016/j.atmosenv.2019.116845, 2019.

Qiao, X., Zhang, Q., Wang, D., Hao, J., and Jiang, J.: Improving data reliability: A quality control practice for low-cost PM(2.5) sensor network, Sci Total Environ, 779, 146381, 10.1016/j.scitotenv.2021.146381, 2021.

Reinecke, T., Leiminger, M., Jordan, A., Wisthaler, A., and Muller, M.: Ultrahigh Sensitivity PTR-MS Instrument with a Well-Defined Ion Chemistry, Anal Chem, 95, 11879-11884, 10.1021/acs.analchem.3c02669, 2023.

Riva, M., Rantala, P., Krechmer, J. E., Peräkylä, O., Zhang, Y., Heikkinen, L., Garmash, O., Yan, C., Kulmala, M., Worsnop, D., and Ehn, M.: Evaluating the performance of five different chemical ionization techniques for detecting gaseous oxygenated organic species, Atmos. Meas. Tech., 12, 2403-2421, 10.5194/amt-12-2403-2019, 2019.

Rolletter, M., Kaminski, M., Acir, I.-H., Bohn, B., Dorn, H.-P., Li, X., Lutz, A., Nehr, S., Rohrer, F., Tillmann, R., Wegener, R., Hofzumahaus, A., Kiendler-Scharr, A., Wahner, A., and Fuchs, H.: Investigation of the α-pinene photooxidation by OH in the atmospheric simulation chamber SAPHIR, Atmos. Chem. Phys., 19, 11635-11649, 10.5194/acp-19-11635-2019, 2019.

Sekimoto, K., Li, S.-M., Yuan, B., Koss, A., Coggon, M., Warneke, C., and de Gouw, J.: Calculation of the sensitivity of proton-transfer-reaction mass spectrometry (PTR-MS) for organic trace gases using molecular properties, Int. J. Mass Spectrom., 421, 71-94, 10.1016/j.ijms.2017.04.006, 2017.

Sheng, J., Zhao, D., Ding, D., Li, X., Huang, M., Gao, Y., Quan, J., and Zhang, Q.: Characterizing the level, photochemical reactivity, emission, and source contribution of the volatile organic compounds based on PTR-TOF-MS during winter haze period in Beijing, China, Atmospheric Research, 212, 54-63, 10.1016/j.atmosres.2018.05.005, 2018.

Sreeram, A., Blomdahl, D., Misztal, P., and Bhasin, A.: High resolution chemical fingerprinting and real-time oxidation dynamics of asphalt binders using Vocus Proton Transfer Reaction (PTR-TOF) mass spectrometry, Fuel, 320, 10.1016/j.fuel.2022.123840, 2022.

Thomas, S. J., Li, H., Praplan, A. P., Hellén, H., and Bianchi, F.: Complexity of downy birch emissions revealed by Vocus proton transfer reaction time-of-flight mass spectrometer, Frontiers in Forests and Global Change, 5, 10.3389/ffgc.2022.1030348, 2022.

Vermeuel, M. P., Novak, G. A., Kilgour, D. B., Claflin, M. S., Lerner, B. M., Trowbridge, A. M., Thom, J., Cleary, P. A., Desai, A. R., and Bertram, T. H.: Observations of biogenic volatile organic compounds over a mixed temperate forest during the summer to autumn transition, Atmos. Chem. Phys., 23, 4123-4148, 10.5194/acp-23-4123-2023, 2023.

https://doi.org/10.5194/egusphere-2024-1325
Preprint. Discussion started: 22 May 2024

Vettikkat, L., Miettinen, P., Buchholz, A., Rantala, P., Yu, H., Schallhart, S., Petäjä, T., Seco, R., Männistö, E., Kulmala, M., Tuittila, E.-S., Guenther, A. B., and Schobesberger, S.: High emission rates and strong temperature response make boreal wetlands a large source of isoprene and terpenes, Atmos. Chem. Phys., 23, 2683-2698, 10.5194/acp-23-2683-2023, 2023.

Wang, L., Slowik, J. G., Tong, Y., Duan, J., Gu, Y., Rai, P., Qi, L., Stefenelli, G., Baltensperger, U., Huang, R.-J., Cao, J., and Prévôt, A. S. H.: Characteristics of wintertime VOCs in urban Beijing: Composition and source apportionment, Atmospheric Environment: X, 9, 10.1016/j.aeaoa.2020.100100, 2021.

Wang, M., Chen, D., Xiao, M., Ye, Q., Stolzenburg, D., Hofbauer, V., Ye, P., Vogel, A. L., Mauldin, R. L., 3rd, Amorim, A., Baccarini, A., Baumgartner, B., Brilke, S., Dada, L., Dias, A., Duplissy, J., Finkenzeller, H., Garmash, O., He, X. C., Hoyle, C. R., Kim, C., Kvashnin, A., Lehtipalo, K., Fischer, L., Molteni, U., Petaja, T., Pospisilova, V., Quelever, L. L. J., Rissanen, M., Simon, M., Tauber, C., Tome, A., Wagner, A. C., Weitz, L., Volkamer, R., Winkler, P. M., Kirkby, J., Worsnop, D. R., Kulmala, M., Baltensperger, U., Dommen, J., El-Haddad, I., and Donahue, N. M.: Photo-oxidation of Aromatic Hydrocarbons Produces Low-Volatility Organic Compounds, Environ Sci Technol, 54, 7911-7921, 10.1021/acs.est.0c02100, 2020a.

Wang, W., Yuan, B., Su, H., Cheng, Y., Qi, J., Wang, S., Song, W., Wang, X., Xue, C., Ma, C., Bao, F., Wang, H., Lou, S., and Shao, M.: A large role of missing volatile organic compound reactivity from anthropogenic emissions in ozone pollution regulation, Atmos. Chem. Phys., 24, 4017-4027, 10.5194/acp-24-4017-2024, 2024.

Wang, Y., Yang, G., Lu, Y., Liu, Y., Chen, J., and Wang, L.: Detection of gaseous dimethylamine using vocus proton-transfer-reaction time-of-flight mass spectrometry, Atmos. Environ., 243, 10.1016/j.atmosenv.2020.117875, 2020b.

Wang, Y., Mehra, A., Krechmer, J. E., Yang, G., Hu, X., Lu, Y., Lambe, A., Canagaratna, M., Chen, J., Worsnop, D., Coe, H., and Wang, L.: Oxygenated products formed from OH-initiated reactions of trimethylbenzene: autoxidation and accretion, Atmos. Chem. Phys., 20, 9563-9579, 10.5194/acp-20-9563-2020, 2020c.

Wennberg, P. O., Bates, K. H., Crounse, J. D., Dodson, L. G., McVay, R. C., Mertens, L. A., Nguyen, T. B., Praske, E., Schwantes, R. H., Smarte, M. D., St Clair, J. M., Teng, A. P., Zhang, X., and Seinfeld, J. H.: Gas-Phase Reactions of Isoprene and Its Major Oxidation Products, Chem. Rev., 118, 3337-3390, 10.1021/acs.chemrev.7b00439, 2018.

Williams, J. and Koppmann, R.: Volatile Organic Compounds in the Atmosphere: An Overview, in: Volatile Organic Compounds in the Atmosphere, 1-32, https://doi.org/10.1002/9780470988657.ch1, 2007.

Wohl, C., Güell-Bujons, Q., Castillo, Y. M., Calbet, A., and Simó, R.: Volatile Organic Compounds Released by Oxyrrhis marina Grazing on Isochrysis galbana, Oceans, 4, 151-169, 10.3390/oceans4020011, 2023.

Wu, C., Wang, C., Wang, S., Wang, W., Yuan, B., Qi, J., Wang, B., Wang, H., Wang, C., Song, W., Wang, X., Hu, W., Lou, S., Ye, C., Peng, Y., Wang, Z., Huangfu, Y., Xie, Y., Zhu, M., Zheng, J., Wang, X., Jiang, B., Zhang, Z., and Shao, M.: Measurement report: Important contributions of oxygenated compounds to emissions and chemistry of volatile organic compounds in urban air, Atmos. Chem. Phys., 20, 14769-14785, 10.5194/acp-20-14769-2020, 2020.

Xu, X., Stee, L. L. P., Williams, J., Beens, J., Adahchour, M., Vreuls, R. J. J., Brinkman, U. A., and Lelieveld, J.: Comprehensive two-dimensional gas

https://doi.org/10.5194/egusphere-2024-1325
Preprint. Discussion started: 22 May 2024

chromatography (GC × GC) measurements of volatile organic compounds in the atmosphere, Atmospheric Chemistry & Physics, 3, 665-682, 2003.

Yacovitch, T. I., Lerner, B. M., Canagaratna, M. R., Daube, C., Healy, R. M., Wang, J. M., Fortner, E. C., Majluf, F., Claflin, M. S., Roscioli, J. R., Lunny, E. M., and Herndon, S. C.: Mobile Laboratory Investigations of Industrial Point Source Emissions during the MOOSE Field Campaign, Atmosphere, 14, 10.3390/atmos14111632, 2023.

Yang, X., Wang, H., Lu, K., Ma, X., Tan, Z., Long, B., Chen, X., Li, C., Zhai, T., Li, Y., Qu, K., Xia, Y., Zhang, Y., Li, X., Chen, S., Dong, H., Zeng, L., and Zhang, Y.: Reactive aldehyde chemistry explains the missing source of hydroxyl radicals, Nat Commun, 15, 1648, 10.1038/s41467-024-45885-w, 2024.

Yu, Y., Guo, S., Wang, H., Shen, R., Zhu, W., Tan, R., Song, K., Zhang, Z., Li, S., Chen, Y., and Hu, M.: Importance of Semivolatile/Intermediate-Volatility Organic Compounds to Secondary Organic Aerosol Formation from Chinese Domestic Cooking Emissions, Environ. Sci. Technol., 10.1021/acs.estlett.2c00207, 2022.

Yuan, B., Koss, A. R., Warneke, C., Coggon, M., Sekimoto, K., and de Gouw, J. A.: Proton-Transfer-Reaction Mass Spectrometry: Applications in Atmospheric Sciences, Chem. Rev., 117, 13187-13229, 10.1021/acs.chemrev.7b00325, 2017.

Yuan, B., Koss, A., Warneke, C., Gilman, J. B., Lerner, B. M., Stark, H., and de Gouw, J. A.: A high-resolution time-of-flight chemical ionization mass spectrometer utilizing hydronium ions (H3O+ ToF-CIMS) for measurements of volatile organic compounds in the atmosphere, Atmos. Meas. Tech., 9, 2735-2752, 10.5194/amt-9-2735-2016, 2016.

Yuan, Q., Zhang, Z., Chen, Y., Hui, L., Wang, M., Xia, M., Zou, Z., Wei, W., Ho, K. F., Wang, Z., Lai, S., Zhang, Y., Wang, T., and Lee, S.: Origin and transformation of volatile organic compounds at a regional background site in Hong Kong: Varied photochemical processes from different source regions, Sci Total Environ, 168316, 10.1016/j.scitotenv.2023.168316, 2023.

Zaytsev, A., Breitenlechner, M., Koss, A. R., Lim, C. Y., Rowe, J. C., Kroll, J. H., and Keutsch, F. N.: Using collision-induced dissociation to constrain sensitivity of ammonia chemical ionization mass spectrometry (NH4+ CIMS) to oxygenated volatile organic compounds, Atmos Meas Tech, 12, 1861-1870, 10.5194/amt-12-1861-2019, 2019a.

Zaytsev, A., Koss, A. R., Breitenlechner, M., Krechmer, J. E., Nihill, K. J., Lim, C. Y., Rowe, J. C., Cox, J. L., Moss, J., Roscioli, J. R., Canagaratna, M. R., Worsnop, D. R., Kroll, J. H., and Keutsch, F. N.: Mechanistic study of the formation of ring-retaining and ring-opening products from the oxidation of aromatic compounds under urban atmospheric conditions, Atmos Chem Phys, 19, 15117-15129, 10.5194/acp-19-15117-2019, 2019b.

Zhang, Y., Xu, W., Zhou, W., Li, Y., Zhang, Z., Du, A., Qiao, H., Kuang, Y., Liu, L., Zhang, Z., He, X., Cheng, X., Pan, X., Fu, Q., Wang, Z., Ye, P., Worsnop, D. R., and Sun, Y.: Characterization of organic vapors by a Vocus proton-transfer-reaction mass spectrometry at a mountain site in southeastern China, Sci Total Environ, 919, 170633, 10.1016/j.scitotenv.2024.170633, 2024.

Zhao, J. and Zhang, R.: Proton transfer reaction rate constants between hydronium ion (H3O+) and volatile organic compounds, Atmos. Environ., 38, 2177-2185, 10.1016/j.atmosenv.2004.01.019, 2004.